

pubs.acs.org/Macromolecules Article

Influence of Molecular Architecture on the Viscoelastic Properties of Polymers with Phase-Separated Dynamic Bonds

Peyton Carden, Sirui Ge, Sheng Zhao, Bingrui Li, Subarna Samanta, and Alexei P. Sokolov*



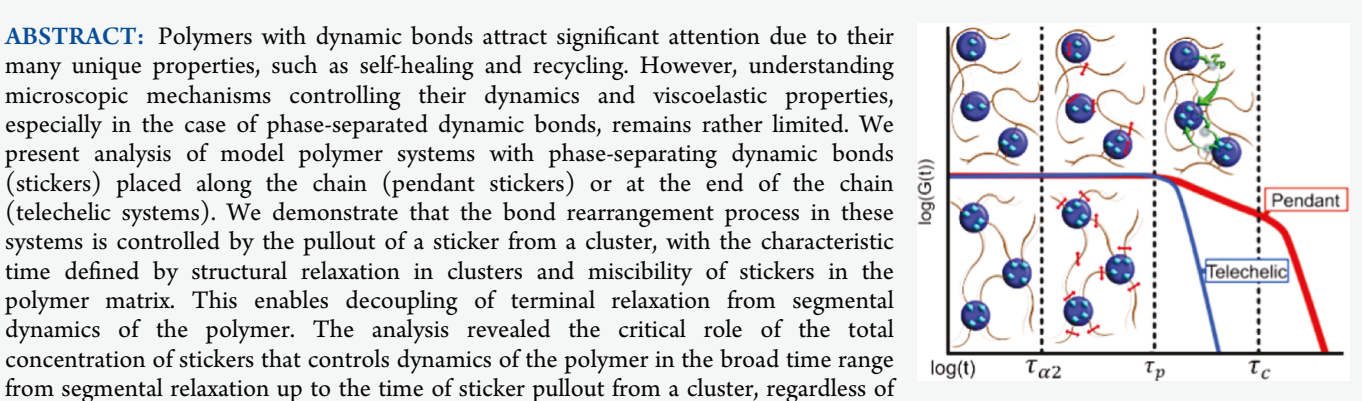
Cite This: Macromolecules 2023, 56, 5173-5180



ACCESS

III Metrics & More

ABSTRACT: Polymers with dynamic bonds attract significant attention due to their many unique properties, such as self-healing and recycling. However, understanding microscopic mechanisms controlling their dynamics and viscoelastic properties, especially in the case of phase-separated dynamic bonds, remains rather limited. We present analysis of model polymer systems with phase-separating dynamic bonds (stickers) placed along the chain (pendant stickers) or at the end of the chain (telechelic systems). We demonstrate that the bond rearrangement process in these systems is controlled by the pullout of a sticker from a cluster, with the characteristic time defined by structural relaxation in clusters and miscibility of stickers in the polymer matrix. This enables decoupling of terminal relaxation from segmental dynamics of the polymer. The analysis revealed the critical role of the total concentration of stickers that controls dynamics of the polymer in the broad time range



Article Recommendations

the sticker placement on the chain and the length of the chain. Only at longer time scales, the molecular length and sticker placement influence viscoelastic properties. Based on these results, we suggest a general scenario for mechanisms controlling the dynamics and viscoelasticity of polymers with phase-separated dynamic bonds. This scenario can be helpful in guiding the design of dynamic polymers with desired viscoelastic properties.

INTRODUCTION

Polymers have now penetrated all levels of our life, and the volume of their production combined with their low recyclability has resulted in significant ecological problems and pollution. One of the potential ways to resolve this problem is design of polymers with reversible (dynamic) bonds. 1-3 This will enable much easier recyclability of polymers. Moreover, polymers with dynamic bonds have many properties not available for traditional polymers, including self-healing, shape-memory, and time-programable properties. 4-10 Inserting dynamic bonds enables an additional multitude of design parameters targeting unique mechanical and viscoelastic properties. However, understanding detailed molecular mechanisms controlling the viscoelasticity of polymers with dynamic bonds remains a challenge.

Properties of polymers with dynamic bonds (we will call them stickers) can be varied based on the sticker type (Hbonding, dynamic covalent, ionic, etc.), its bond strength, concentration, placement on the polymer chain (telechelic, pendant, multi-arm, etc.), and even on the miscibility between stickers and the polymer matrix. Low miscibility of the stickers will lead to their phase separation and formation of clusters of stickers. This is well known for polymers with ionic and hydrogen bonds, and recently it was also demonstrated for some systems with dynamic covalent bonds. 11,12 It has been shown that viscoelastic properties and terminal relaxation of these systems are controlled by structural relaxation in the clusters of stickers and not by the segmental dynamics of the polymer. 13-15 This enables a separate control of elasticity and terminal relaxation/viscosity of the system, opening an alternative way to design recyclable elastomers. These systems will behave as regular crosslinked systems (thermosets) at temperatures below the glass transition temperature, $T_{\rm g}$, of the clusters, while they can be easily recycled at temperatures above this $T_{\rm g}$.

The sticky Rouse and sticky reptation models 16,17 have been actively employed to describe the behavior of polymers with dynamic bonds, including systems with phase-separated stickers (see, e.g., ref 18). These models, however, do not consider the detailed microscopic mechanism of bond rearrangements in the specific case of phase-separated dynamic bonds. Theoretical analysis presented in ref 19 suggested that the bond exchange mechanism in systems with phase-separated stickers should occur through fusion and separation of the

Received: January 6, 2023 Revised: May 8, 2023 Published: May 26, 2023





Figure 1. Structure of a pendant sample with the various molar ratios of stickers (a) and of the earlier studied telechelic samples (b).

Table 1. Parameters of the Polymers Studied Here with Pendant Stickers: m – Number of Non-functionalized Monomers in a Polymer; n – Number of Stickers Per Molecule; $f_{\rm e}$ – Weight Fraction of Stickers; $T_{\rm g}$ of the PDMS Backbone and $T_{\rm g}$ of Clusters; Distance between Centers of Clusters d and Cluster Radius $R_{\rm cluster}^{a}$

	pendant			telechelic				
	DP70	DP100	DP670	DP13	DP19	DP22	DP50	DP74
m/n	64/4	95/5	629/45	11/2	17/2	20/2	48/2	72/2
$f_{ m e}$	0.11	0.09	0.12	0.247	0.184	0.163	0.079	0.057
$T_{\rm g}$ backbone (K)	151	148	151	156	153	151	148	146
T _g clusters (K)	193.5	185	194.5	209	205	193.5	186.5	190
d (nm)	3.87	4.25	3.97	4.08	4.47	4.43	5.12	5.97
$R_{\rm cluster}$ (nm)	1.16	1.13	1.19	1.59	1.58	1.5	1.36	1.43

^aThe same parameters for telechelic polymers with the same stickers are from refs 13, 25, 26.

clusters. However, this mechanism was questioned in experimental studies presented in refs 14 and 20. Our recent studies of telechelic systems with phase-separated dynamic bonds revealed that the bond exchange mechanism (i.e., terminal relaxation in this case) most probably goes through a pulling of individual stickers from the clusters, and it is controlled by the structural relaxation in these clusters and the energy barrier defined by their miscibility in the polymer matrix.¹³ However, these studies were performed on telechelic systems, and the role of molecular architecture and placement of stickers on the chain remains unknown. Several recent simulation studies of telechelic and star-like polymers with stickers revealed specific details of linear and non-linear rheological properties of these systems.^{21–23} These simulations also suggested that an increase in the energy of the stickers interactions up to ~5RT will lead to their phase separation from the polymer matrix for both, linear and star chains.²³

The present study focuses on revealing the role of placement of stickers as pendant groups along the chain with different molecular weights on the dynamics and viscoelastic properties of polymers with phase-separated stickers. We chose polydimethylsiloxane (PDMS) with pendant groups bearing phase-separating hydrogen bonding functionalities as a model system and compared the results with earlier studies of telechelic PDMS with the same functional groups. The interaction strength for this particular functionality was estimated in the previous work to be ~14 kJ/mol. Smallangle X-ray scattering (SAXS) was employed to characterize structure, while broadband dielectric spectroscopy (BDS) and rheology were employed to characterize the dynamics and viscoelastic properties of these systems. Our results revealed that the concentration of stickers appears to be the

important parameter controlling the dynamics of these systems in a broad frequency range from segmental relaxation to the dynamic bond rearrangement (a single sticker pullout), regardless of sticker placement on the chain. Only on time scales longer than the bond rearrangement does the difference in molecular weight and architecture play a role. We demonstrate that this behavior can be explained by the earlier developed model for telechelic systems ¹³ combined with the sticky Rouse model. Although the model system in this study is based on hydrogen bonding, the developed understanding is applicable to systems with other types of dynamic bonds and provides a guidance for the design of novel functional materials with desired viscoelastic properties and recyclability.

MATERIALS AND METHODS

Synthesis of Pendant Polymers. Aminopropylmethylsiloxane—dimethylsiloxane copolymers with labeled molecular weights of 4000–5000 (~6% functionalized repeat units), 7000–9000 (~5% functionalized repeat units), and 50,000 g/mol (~7% functionalized repeat units), respectively, were purchased from Gelest, Inc. 4-(Dimethylamino)pyridine (DMAP) and succinic anhydride were purchased from Sigma-Aldrich; dichloromethane (DCM) and hydrochloric acid (36.5–38%) were purchased from VMR Analytical and used as received. Triethylamine (TEA) was distilled with calcium hydride before use.

The general procedure is based on our earlier work 24,25 with minor change. PDMS-pendant NH $_2$ (AMS-162, 4 g, 1 mmol) and triethylamine (0.607 g, 6 mmol) were dissolved in 25 mL of anhydrous tetrahydrofuran (THF). 4-(Dimethylamino)-pyridine (0.245 g, 2 mmol) and succinic anhydride (0.8 g, 8 mmol) in 10 mL of anhydrous THF were added to the PDMS solution. The reaction was performed at 40 °C for 2 days under the protection of a nitrogen atmosphere. After evaporating the organic solvent, 1 mol/L hydrochloric acid solution (40 mL) was added, and the mixture was

stirred for 3 h. DCM was used to extract the product (30 mL) and then washed with deionized water three times (10 mL \times 3). The organic layer was collected and then purified by dialysis over DCM, and dried in a vacuum oven at 60 °C overnight.

The chemical structure of the obtained PDMS samples with various molar ratios of randomly placed pendant functional groups 4-(propylamino)-4-oxobutanoic acid (COOH) was verified by NMR and is presented in Figure 1. DP presents the degree of polymerization of the backbone. Figure 1 also shows the structure of the earlier studied telechelic PDMS with the same functional groups at chain ends. Various parameters of the studied molecules are presented in Table 1.

X-ray Scattering. DP70, DP100, and DP670 samples were measured on XEUSS 3.0 (Xenocs, France) equipped with a Cu K α microfocus source and a Pilatus 300k detector (Dectris, Switzerland). The scattering wavevector (q) was calibrated by a silver behenate standard material. The distance between sample and detector was 0.9 and 0.55 m for SAXS and WAXS, respectively. The samples were forced into quartz capillaries with a diameter of 1.5 mm and a 0.01 mm wall thickness. These capillaries, as well as an empty reference capillary, were placed perpendicular to the X-ray beam. These measurements were taken at room temperature, and the intensity of the empty reference capillary was subtracted from each sample.

Small-Amplitude Oscillatory Shear Rheology. Small-amplitude oscillatory shear (SAOS) rheological measurements were utilized to probe the viscoelastic properties of pendant functionalized PDMS—COOH through a strain-controlled mode of the AR2000ex (TA Instruments) with an angular frequency range from 10^2 to 10^{-1} rad/s. We used parallel plate geometry with a disk diameter of 4 mm at a variety of temperatures range from T_g of the PDMS backbone to temperatures where the sample can flow freely. The strain amplitude during the measurement was chosen to be in the range from 0.03 to 5%, depending on the modulus level at different temperatures.

Broadband Dielectric Spectroscopy. Dielectric spectra in the frequency range from 10^{-2} to 10^6 Hz were measured utilizing a Novocontrol system, which includes an Alpha-A impedance analyzer and a Quatro Cryosystem temperature control unit. The pendant functionalized PDMS–COOH samples were placed into a parallel plate dielectric cell made of sapphire and invar steel with an electrode diameter of 10 mm and a capacitance of ~2.9 pF with an electrode separation of ~220 μ m. To prevent crystallization, all samples were quenched from room temperature to about 113 K and reheated to 10 K below the $T_{\rm g}$ before the measurements. All the spectra were measured on heating. After each temperature increase, the samples were equilibrated for 10 min to reach thermal stabilization within 0.1 K.

RESULTS

X-ray scattering data (Figure 2) provides information about the morphology of the studied samples. The higher q peak around 0.9 Å⁻¹ is attributed to the PDMS chains themselves, ²⁷ and the presence of functional group aggregation was confirmed for all samples by the low-q peak around 0.1 Å⁻¹. Although cluster size probably has a large distribution in these systems, we can do estimates of some average parameters important for understanding the structure of these systems. The averaged center-to-center distance between the clusters can be estimated using the low-q peak position q_c

$$d \approx 2\pi/q_{\rm c} \tag{1}$$

The peak position q_c was estimated using a Gaussian fit function. Assuming that all functional groups are segregated in the phase-separated clusters, which have a cubic arrangement within the polymer matrix, and their volume fraction is the same as their weight fraction, we can estimate an average radius of the clusters from the volume fraction of the functional groups f_c^{28}

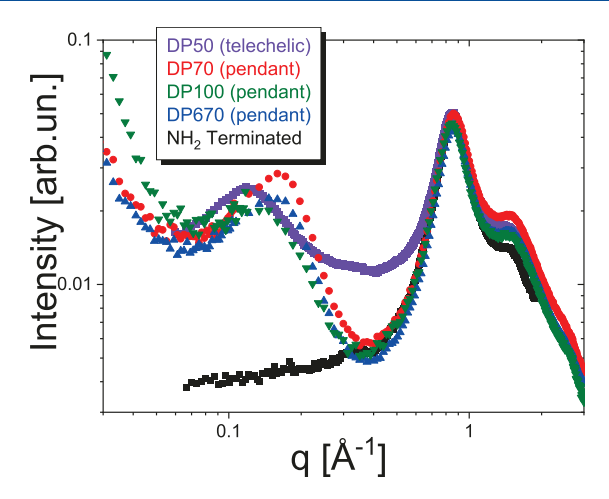


Figure 2. X-ray scattering data for each sample reveals a low-q peak that indicates phase separation. PDMS with no phase separation and no low-q peak is shown as a reference.

$$R_{\text{cluster}} = \frac{d}{2} \left(\frac{6f_{\text{e}}}{\pi} \right)^{1/3} \tag{2}$$

For systems with similar fraction of functional groups, the distance between clusters and cluster radius appear a bit smaller in pendant systems than in telechelic ones (Table 1), most probably due to a smaller chain length between stickers for pendant systems than for telechelic ones at the same f_e .

In agreement with the earlier studies of telechelic PDMS with the same functional end groups, 13,24,25 the BDS spectra for the samples studied here show three processes (Figure 3): (1) a high-frequency process corresponding to segmental motion of the polymer backbone (α process); (2) a low-amplitude process in the intermediate frequency range corresponding to the dissociation of dimeric associating groups (α *); and (3) a low-frequency process corresponding to the mobility of stickers within associating clusters (α ₂).

To estimate the relaxation times of these processes, the permittivity loss spectra were fit to a Havriliak-Negami function

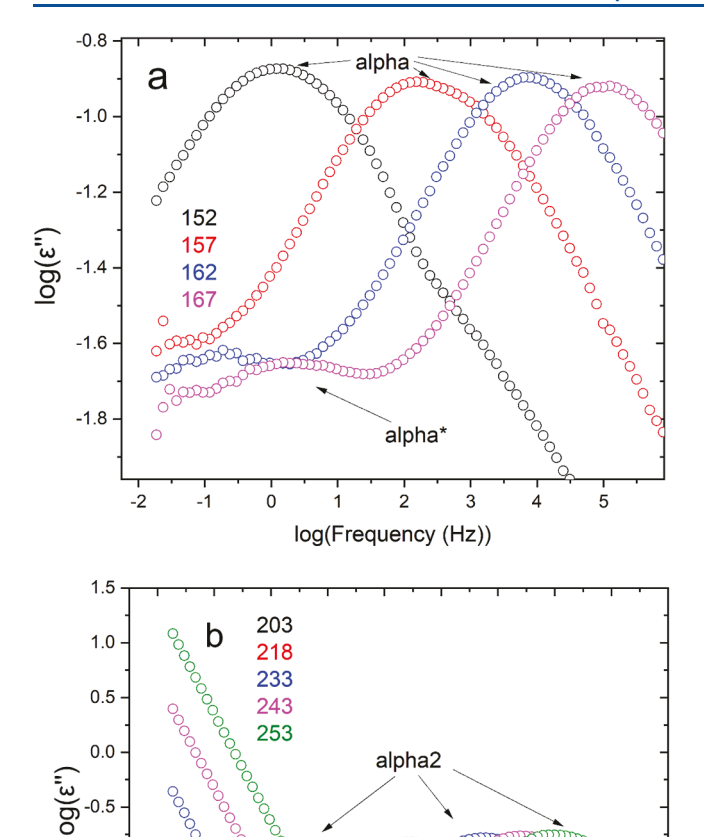
$$\varepsilon''(f) = -Im \frac{\Delta \varepsilon}{(1 + (i2\pi f \tau_{\rm HN})^{\alpha})^{\gamma}}$$
(3)

Here $\Delta \varepsilon$ is the dielectric amplitude of a given process, $\tau_{\rm HN}$ corresponds to the characteristic Havriliak—Negami relaxation time of the process, while α and γ represent shape parameters for the process. Usually the frequency of the loss peak maximum is used to estimate the characteristic relaxation time, and it can be related to the $\tau_{\rm HN}^{29}$

$$\tau_{\text{max}} = \tau_{\text{HN}} \left(\frac{\sin\left(\frac{\pi \alpha \gamma}{2 + 2\gamma}\right)}{\sin\left(\frac{\pi \alpha}{2 + 2\gamma}\right)} \right)^{1/\gamma} \tag{4}$$

By extrapolating the VFT temperature dependence of the α relaxation times to τ = 100 s, the $T_{\rm g}$ of the polymer matrix was calculated. The glass transition temperature of the phase-separated clusters was estimated in the same way using the α_2 relaxation time (Figure 4, Table 1).

SAOS rheology was utilized for studies of the viscoelastic behavior of these samples. The master curves were constructed using time—temperature superposition by matching the data



log(Frequency (Hz))

Figure 3. Dielectric permittivity loss spectra of the DP100 sample at low (a) and high (b) temperatures (K), showing relaxation processes corresponding to the polymer segmental relaxation (alpha), dimeric dissociations (alpha*), and relaxation in clusters (alpha2).

-1.5

-2.0

measured at different temperatures (Figure 5). Although time-temperature superposition quantitatively fails in the case of these samples due to a strong difference in temperature dependence of segmental and terminal relaxation (Figure 4), the master curves provide a useful qualitative picture of the viscoelastic behavior. All the master curves show segmental relaxation at higher frequencies that is followed by a rubbery plateau with modulus $G_{\rm N}$ ~1-4 MPa at intermediate frequencies (Figure 5). The DP 100 sample demonstrates a lower plateau modulus in part due to its larger molecular weight between sticker groups. Additional reinforcement for samples with DP 70 and DP 670 came from the interfacial polymer layer with higher mechanical modulus formed around clusters and a relatively short distance between cluster surfaces, d_{IPS} . The latter can be roughly estimated as $d_{\text{IPS}} = d$ $2R_{\text{cluster}}$ (see Table 1) and is ~1.55–1.6 nm for DP 70 and DP 670 samples, and ~2 nm for DP 100 sample. According to our earlier studies, ²⁴ the thickness of the interfacial polymer layer in telechelic systems with clusters of the same stickers is \sim 0.7–0.9 nm. Thus, the interfacial layers almost overlap in the DP 70 and DP 670 samples, leading to three times higher

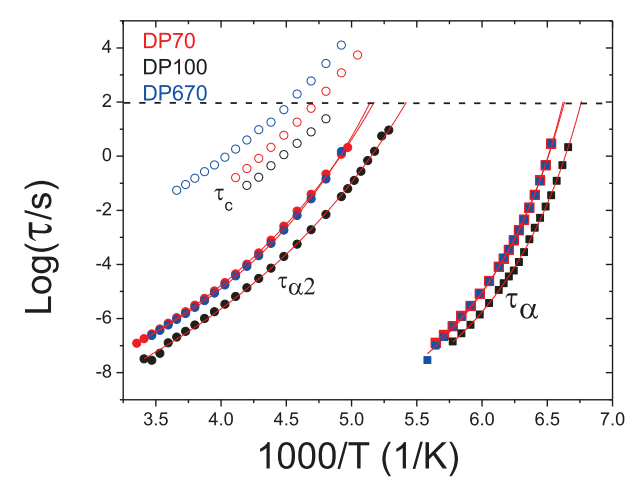


Figure 4. Temperature dependence of characteristic relaxation times for the α - and α_2 -processes estimated from the dielectric spectra (closed symbols) and terminal relaxation time (τ_C , open symbols) estimated from rheology for studied systems with pendant stickers. Solid lines show VFT fits and their crossing point with the dashed line corresponding to $\tau=100$ s is taken as T_g .

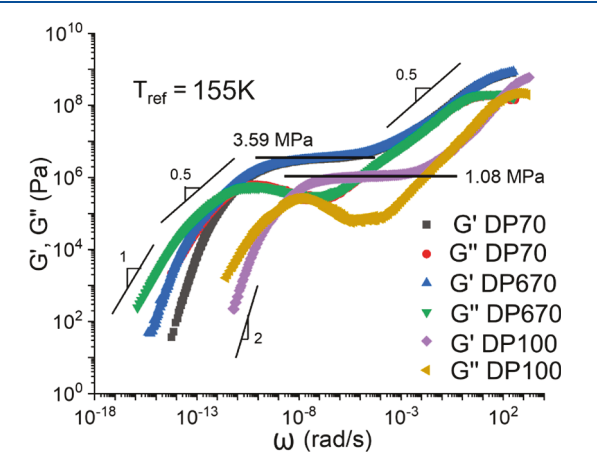


Figure 5. Rheological master curve for each pendant functionalized sample. The spectra of DP70 and DP670 coincide up to the frequency of the loss modulus maximum below the end of the rubbery plateau.

plateau modulus than in the DP 100 sample (Figure 5). The DP 100 sample also exhibits the fastest segmental and terminal relaxation times due to the lower weight fraction of sticker groups.

At lower frequencies, a power law dependence with $G'(\omega) \sim G''(\omega) \propto \omega^{0.5}$ is clearly observed for all the samples, and then terminal relaxation appears at still lower frequency. This behavior can be well described by using the Rouse equations (Figure 6)³⁰

$$G' = G_0 \sum_{j=1}^{N} \frac{\omega^2 \tau_j^2}{1 + \omega^2 \tau_j^2} \text{ and } G'' = G_0 \sum_{j=1}^{N} \frac{\omega \tau_j}{1 + \omega^2 \tau_j^2}$$
 (5)

With $\tau_j = \tau_c/j^2$, where τ_c is the terminal relaxation time and N is the number of sticky Rouse modes. The fit of the master curves provided estimates of τ_c (Figure 4) and the shortest $\tau_j = \tau_N = \tau_p$ which marks the onset of the sticky Rouse regime, i.e., the beginning of the rubbery plateau softening. The fit using eq 5 does not describe high-frequency data well (Figure 6), probably due to additional higher-frequency modes. This fit, however, provides good estimates of the characteristic

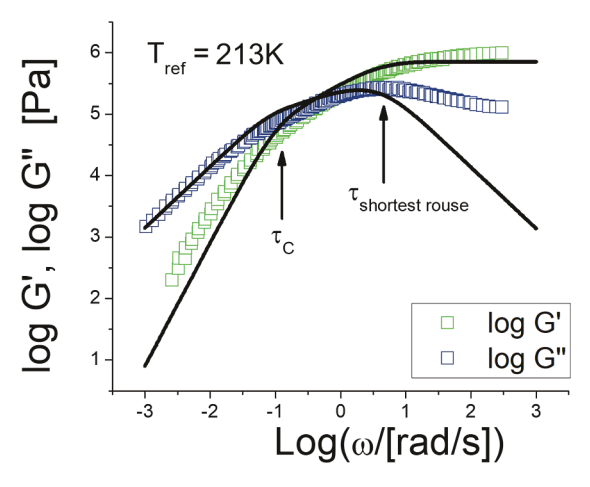


Figure 6. Rheological data for the DP100 sample (symbols) and their fit to the Rouse model eq 5 (lines). Arrows indicate two characteristic time scales extracted from the fit.

relaxation times. We emphasize that the temperature dependence of these characteristic times is estimated only when the sticky Rouse regime is in the frequency window of the rheometer. In this way, we avoided any inaccuracy due to a breakdown of time-temperature superposition potentially encountered through a construction of the master plots (Figure 5).

DISCUSSION

To unravel the role of molecular architecture and the placement of stickers on the chain, we will compare the obtained results to the data on telechelic PDMS–COOH samples with different DPs studied in our earlier publications. 13,24,25 We start with an analysis of $T_{\rm g}$ of these systems. Recent theoretical work 26 suggested that the shift of $T_{\rm g}$ in polymers with stickers should follow a roughly linear increase with the fraction of stickers, regardless of whether stickers are only at the chain ends (telechelic systems) or are placed randomly along the chain. Our data (Figure 7) indeed are consistent with this theoretical prediction and reveal that

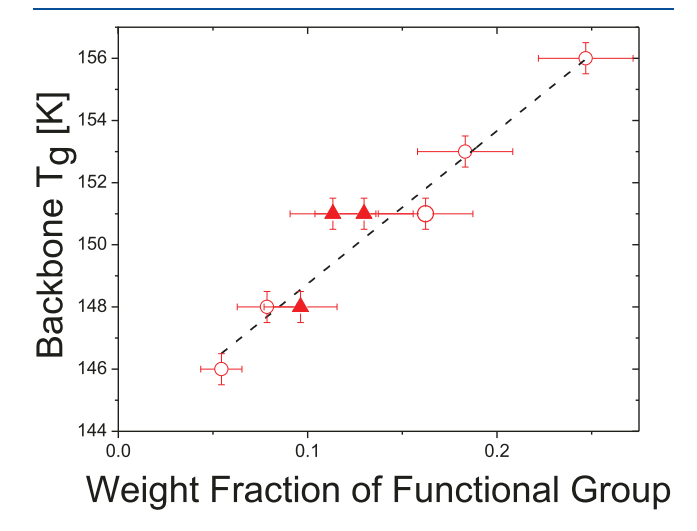


Figure 7. Dependence of the glass transition temperature $T_{\rm g}$ on the weight fraction of the functional group for telechelic (open circles) and pendant (closed triangles) PDMS-COOH systems. Data for telechelic systems are from ref 26.

regardless of the chain length and placement of the stickers, their fraction seems to define the system's $T_{\rm g}$. Although the pendant samples studied here do not cover a broad range of sticker concentration, they vary by more than a factor of 10 in molecular weight, and their segmental behavior agrees well with the broader body of data available for telechelic systems. This result emphasizes the importance of the changes in segmental dynamics and $T_{\rm g}$ with increasing concentrations of stickers. We want to stress that these changes are usually not considered in sticky Rouse or sticky reptation models, although they strongly affect segmental friction of these systems.

The slowest dielectric process marked as α_2 -process corresponds to structural relaxation in clusters of stickers. ^{13,25} To reveal how the process of structural relaxation in clusters affects the viscoelastic properties of the studied materials, we compare rheological and dielectric modulus data. This is necessary for a correct comparison of the dielectric and rheological time scales, ^{29,31} as the dielectric permittivity is an experimental response analogous to shear compliance rather than shear modulus. The dielectric loss modulus spectra, $M''(\omega) = Im[1/\varepsilon^*(\omega)]$, were fit to an HN function, and the characteristic relaxation time $\tau_{\rm a2M}$ was estimated from the obtained $\tau_{\rm HN}$ using eq 4. Analysis of the data revealed that in all the samples, the dielectric $\tau_{\rm a2M}(T)$ is shorter than the rheological $\tau_{\rm p}(T)$ by about one order (Figure 8). These results are similar to the earlier studies of telechelic PDMS with the

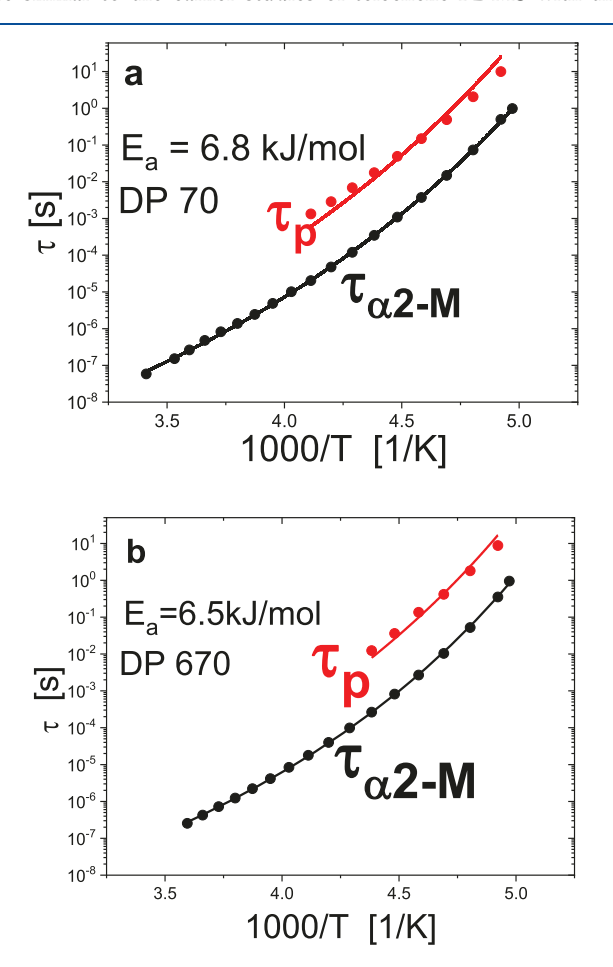


Figure 8. Activation plot for the DP70 (a) and DP670 (b) samples demonstrating the disparity of the dielectric cluster relaxation times $(\tau_{a2\text{-M}})$ with the rheological bond rearrangement time (τ_p) , which indicates the onset of Rouse-like dynamics.

same functional group,¹³ suggesting that the structural relaxation in clusters is not sufficient for sticker rearrangement between clusters. To explain this difference, we adopt the idea from our previous work, where the additional factor controlling rearrangement of stickers between clusters is the difference in miscibility between the bulk polymer matrix and functional groups. This idea is based on their similarity to block copolymers.^{32–35} In this case, the onset of the rubbery plateau softening should be related to the characteristic time of pulling a sticker from a cluster and can be described using the following equation¹³

$$\tau_{\rm p} = \tau_{\alpha 2-{\rm M}} {\rm exp} \left(\frac{E_{\rm a}}{RT} \right) = \tau_{\alpha 2-{\rm M}} {\rm exp} (\alpha \chi N_{\rm core})$$
 (6)

Here $E_{\rm a}$ corresponds to the activation energy barrier necessary to overcome the miscibility difference of the stickers and polymer matrix described by the Flory–Huggins solubility parameter χ , $N_{\rm core}=1$ in the case of our stickers. The eq 6 describes well the temperature dependence of $\tau_{\rm p}$ (Figure 8) and provides an estimate of $E_{\rm a}\sim 6.7\pm 0.5$ kJ/mol, in good agreement with our previous studies of telechelic PDMS with the same stickers (~ 6.6 kJ/mol). It was demonstrated in ref 13 that this value agrees well with estimates of the Flory–Huggins parameter using the Hansen solubility parameter approach. 36,37

Direct comparison of the rheological data for the DP 100 sample with pendant stickers to those of the DP50 telechelic sample (Figure 9), which have approximately the same volume

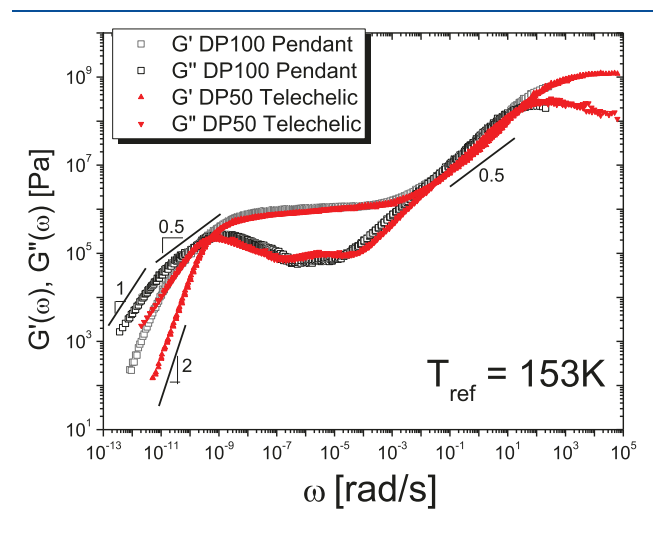


Figure 9. Comparison of the shear modulus spectra of the DP100 sample with pendant functional groups (black open symbols) to the spectra of the telechelic DP50 sample (red symbols). Lines mark the power law regions with the slope indicated by numbers.

fraction of stickers (Table 1), clearly reveals the impact of sticker placement on the viscoelasticity of a polymer with phase-separated functional groups. While in telechelic systems, pulling a sticker out of a cluster results in terminal relaxation, i.e., $\tau_c \sim \tau_p$, an extended softening regime with a Rouse-like behavior appears in the rheological data of the system with stickers placed along the chain (Figure 9). In the latter case, the terminal relaxation time appears significantly slower than the τ_p (Figure 9), and the difference between these time scales increases with the increase of molecular weight of the chain at approximately the same fraction of stickers placed along the chain (Figure 4). This behavior is well explained by the sticky

Rouse model, as stickers placed along the chain slow down the Rouse modes by the time of sticker pullout, and the terminal relaxation is then defined by the slowest sticky Rouse mode. The influence of sticker placement becomes even more apparent from direct comparison of relaxation times for samples with comparable fraction of stickers (Figure 10). The

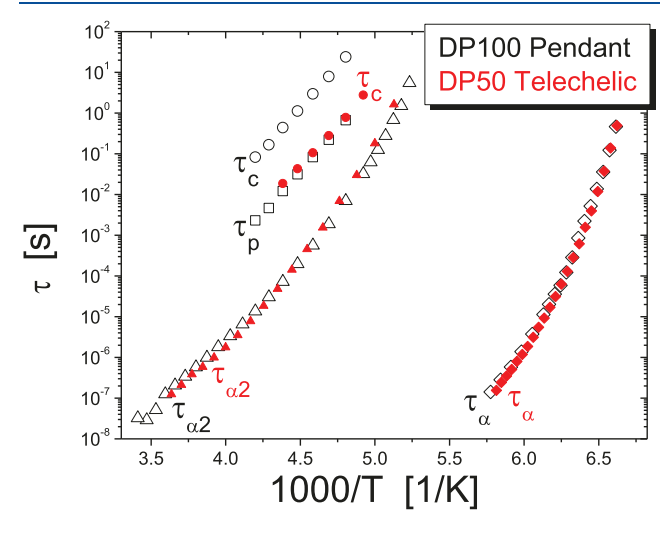


Figure 10. Comparison of dielectric and rheological relaxation times for systems with the same fraction of stickers: DP100 with pendant stickers (black open symbols) and DP50 with a telechelic sample (red symbols).

two architectures show good agreement in their segmental (α) and cluster (α_2) relaxation times, and even their sticker pullout times appear to be the same (Figure 10). This suggests that the volume fraction of the functional group is the major parameter controlling these times and the viscoelastic properties of these systems up to the time of pulling a sticker from a cluster, regardless of the sticker's placement in these systems. The difference appears only at longer time scales: while pulling a sticker from a cluster results in terminal relaxation for telechelic systems, the same event results in the onset of sticky Rouse dynamics in the systems with stickers placed along the chain.

Based on these results, we propose the following general scenario for the viscoelastic properties of polymers with microphase-separated stickers. Attaching stickers to a polymer chain leads to a slowdown of segmental relaxation and an increase in T_g due to the temporary crosslinks introduced by stickers. T_g increases roughly linearly with the concentration of stickers, regardless of their placement on the chain²⁶ (Figure 7). Clusters of stickers lead to an extended rubbery plateau even in systems with relatively short chains (Figure 5). Clusters also provide reinforcement of the rubbery plateau level, 13,38 the effect similar to the one known for polymer nanocomposites. Especially strong reinforcement appears in the case of percolating interfacial layers as was demonstrated in. 13 Structural relaxation in clusters (the α_2 process) detected in the dielectric spectra is visible in rheological data only for percolated systems. It appears as the onset of softening of the extremely high rubbery plateau. 13 In all other systems, rheological data do not detect the structural relaxation in clusters, and instead detect the events of sticker pullout from a cluster (Figure 11). In simple terms, viscoelastic properties are sensitive to the rearrangements of stickers between different clusters. This process is controlled by structural relaxation in

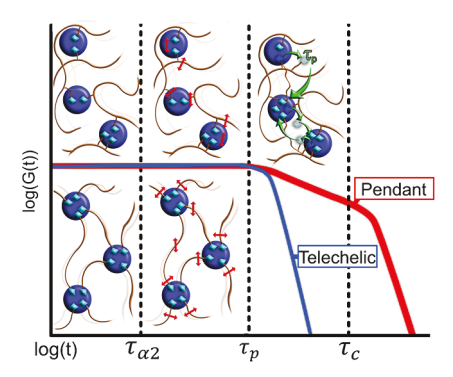


Figure 11. Cartoon depicting the regimes of viscoelastic behavior for pendant functionalized and telechelically functionalized associating systems with microphase separation. The stickers are frozen in the clusters until time $\tau_{\alpha 2}$, they are moving inside the clusters at times longer than $\tau_{\alpha 2}$ and pulling out from the clusters, providing bond exchange between clusters at time $\tau_{\rm p}$. This time corresponds to terminal relaxation in telechelic systems but appears as the onset of a sticky Rouse regime for systems with pendant stickers. Their terminal relaxation time is defined by the longest sticky Rouse mode.

clusters and the additional energy barrier defined by the Flory—Huggins interaction parameter of the stickers with the polymer matrix (eq 6). It appears that up to this point, the placement of stickers in the chain (telechelic or pendant along the chain) does not play any significant role in the dynamics of the polymer with microphase-separated stickers. Dynamics up to this point depend only on the total concentration of the stickers. The difference, however, appears at longer time scales, where pulling the sticker from the cluster results in terminal relaxation for telechelic systems, while it leads to the onset of sticky Rouse dynamics in the case of stickers placed along the chain (Figures 9–11).

CONCLUSIONS

We presented detailed studies of the dynamics and viscoelastic properties of model polymeric systems with microphase-separated dynamic bonds (stickers). Combined dielectric and rheological data revealed several dynamic processes, including backbone segmental relaxation, structural relaxation in clusters of stickers, the process of sticker pullout from a cluster (the dynamic bond rearrangement process), and terminal relaxation. The most interesting observation is that the dynamics and viscoelastic properties of these materials up to the time of sticker pullout appear to be dependent only on the concentration of stickers and not on their placement on the chain or the molecular weight of the chain. Only at longer time scales do the sticker placement and total molecular weight of the chain with pendant stickers begin to affect the viscoelastic properties of the material.

Based on these results, we propose a general scenario of the viscoelastic properties of the polymers with microphase-separated dynamic bonds. This scenario covers all dynamics starting from segmental relaxation through the terminal regime. It emphasizes the importance of structural relaxation (e.g., $T_{\rm g}$) of dynamic bond clusters, their miscibility with the polymer matrix, and molecular architecture in the viscoelastic properties of these materials. The results demonstrate a clear decoupling of terminal relaxation of these systems from the polymer segmental dynamics. Terminal relaxation in this case is defined by the structural relaxation in clusters of stickers, stickers miscibility in the polymer matrix and their number

along the chain. This enables an independent tuning of the terminal relaxation and elasticity of the system. The use of telechelic polymers enables much faster terminal relaxation with the rest of the dynamics being unaffected. Based on these results, we suggest that the use of telechelic polymers with phase-separated stickers provides the best solution for the design of recyclable elastomers. They will behave as regular thermosets at temperatures below $T_{\rm g}$ of clusters of stickers and provide relatively fast rearrangements at temperatures above this $T_{\rm g}$. Although current experiments were done on systems with hydrogen bonding functionalities, we expect that they are applicable to any other type of dynamic bond that phase-separates from the polymer backbone. This scenario can be instrumental in the design of polymers containing dynamic bonds with desired viscoelastic properties.

AUTHOR INFORMATION

Corresponding Author

Alexei P. Sokolov — Department of Chemistry, University of Tennessee, Knoxville, Tennessee 37996, United States; Chemical Sciences Division, Oak Ridge National Laboratory, Oak Ridge, Tennessee 37830, United States; orcid.org/ 0000-0002-8187-9445; Email: sokolov@utk.edu

Authors

Peyton Carden — Department of Chemistry, University of Tennessee, Knoxville, Tennessee 37996, United States; orcid.org/0000-0001-6229-6538

Sirui Ge − Department of Chemistry, University of Tennessee, Knoxville, Tennessee 37996, United States; ocid.org/ 0000-0002-4276-7838

Sheng Zhao – Department of Chemistry, University of Tennessee, Knoxville, Tennessee 37996, United States

Bingrui Li — The Bredesen Center for Interdisciplinary Research and Graduate Education, University of Tennessee, Knoxville, Tennessee 37996, United States; ◎ orcid.org/ 0000-0002-4974-5826

Subarna Samanta — Department of Chemistry, University of Tennessee, Knoxville, Tennessee 37996, United States;
orcid.org/0000-0003-3386-5556

Complete contact information is available at: https://pubs.acs.org/10.1021/acs.macromol.3c00034

Notes

The authors declare no competing financial interest.

ACKNOWLEDGMENTS

We thank the NSF Polymer Program for the financial support of these studies under award DMR-1904657. X-ray measurements were enabled by the Major Research Instrumentation program of the National Science Foundation under Award no. DMR-1827474.

REFERENCES

- (1) Zheng, N.; Xu, Y.; Zhao, Q.; Xie, T. Dynamic Covalent Polymer Networks: A Molecular Platform for Designing Functions beyond Chemical Recycling and Self-Healing. *Chem. Rev.* **2021**, *121*, 1716–1745.
- (2) Qin, B.; Zhang, S.; Sun, P.; Tang, B.; Yin, Z.; Cao, X.; Chen, Q.; Xu, J. F.; Zhang, X. Tough and Multi-Recyclable Cross-Linked Supramolecular Polyureas via Incorporating Noncovalent Bonds into Main-Chains. *Adv. Mater.* **2020**, *32*, 2000096.

- (3) Cordier, P.; Tournilhac, F.; Soulié-Ziakovic, C.; Leibler, L. Selfhealing and thermoreversible rubber from supramolecular assembly. *Nature* **2008**, *451*, 977–980.
- (4) Li, C.-H.; Wang, C.; Keplinger, C.; Zuo, J.-L.; Jin, L.; Sun, Y.; Zheng, P.; Cao, Y.; Lissel, F.; Linder, C.; et al. A highly stretchable autonomous self-healing elastomer. *Nat. Chem.* **2016**, *8*, 618–624.
- (5) Cao, P.-F.; Li, B.; Hong, T.; Townsend, J.; Qiang, Z.; Xing, K.; Vogiatzis, K. D.; Wang, Y.; Mays, J. W.; Sokolov, A. P.; et al. Superstretchable, Self-Healing Polymeric Elastomers with Tunable Properties. *Adv. Funct. Mater.* **2018**, 28, 1800741.
- (6) Peng, W.; Zhang, G.; Zhao, Q.; Xie, T. Autonomous Off-Equilibrium Morphing Pathways of a Supramolecular Shape-Memory Polymer. *Adv. Mater.* **2021**, *33*, 2102473.
- (7) Cooper, C. B.; Nikzad, S.; Yan, H.; Ochiai, Y.; Lai, J.-C.; Yu, Z.; Chen, G.; Kang, J.; Bao, Z. High Energy Density Shape Memory Polymers Using Strain-Induced Supramolecular Nanostructures. *ACS Cent. Sci.* **2021**, *7*, 1657–1667.
- (8) Luo, J.; Demchuk, Z.; Zhao, X.; Saito, T.; Tian, M.; Sokolov, A. P.; Cao, P.-F. Elastic vitrimers: Beyond thermoplastic and thermoset elastomers. *Matter* **2022**, *5*, 1391–1422.
- (9) Samanta, S.; Kim, S.; Saito, T.; Sokolov, A. P. Polymers with Dynamic Bonds: Adaptive Functional Materials for a Sustainable Future. *J. Phys. Chem. B* **2021**, *125*, 9389–9401.
- (10) Li, B.; Cao, P.-F.; Saito, T.; Sokolov, A. P. Intrinsically Self-Healing Polymers: From Mechanistic Insight to Current Challenges. *Chem. Rev.* **2023**, *123*, 701–735.
- (11) Zhou, X.; Gong, Z.; Fan, J.; Chen, Y. Self-healable, recyclable, mechanically tough transparent polysiloxane elastomers based on dynamic microphase separation for flexible sensor. *Polymer* **2021**, 237, 124357.
- (12) Zhang, W.; Wang, M.; Zhou, J.; Sheng, Y.; Xu, M.; Jiang, X.; Ma, Y.; Lu, X. Preparation of room-temperature self-healing elastomers with high strength based on multiple dynamic bonds. *Eur. Polym. J.* **2021**, *156*, 110614.
- (13) Ge, S.; Samanta, S.; Li, B.; Carden, G. P.; Cao, P.-F.; Sokolov, A. P. Unravelling the Mechanism of Viscoelasticity in Polymers with Phase-Separated Dynamic Bonds. *ACS Nano* **2022**, *16*, 4746–4755.
- (14) Mordvinkin, A.; Suckow, M.; Böhme, F.; Colby, R. H.; Creton, C.; Saalwächter, K. Hierarchical Sticker and Sticky Chain Dynamics in Self-Healing Butyl Rubber Ionomers. *Macromolecules* **2019**, *52*, 4169–4184.
- (15) Tress, M.; Xing, K.; Ge, S.; Cao, P.; Saito, T.; Sokolov, A. What dielectric spectroscopy can tell us about supramolecular networks*. *Eur. Phys. J. E* **2019**, *42*, 133.
- (16) Leibler, L.; Rubinstein, M.; Colby, R. H. Dynamics of reversible networks. *Macromolecules* **1991**, *24*, 4701–4707.
- (17) Rubinstein, M.; Semenov, A. N. Dynamics of Entangled Solutions of Associating Polymers. *Macromolecules* **2001**, 34, 1058–1068.
- (18) Chen, Q.; Tudryn, G. J.; Colby, R. H. Ionomer dynamics and the sticky Rouse model. J. Rheol. 2013, 57, 1441–1462.
- (19) Amin, D.; Likhtman, A. E.; Wang, Z. Dynamics in Supramolecular Polymer Networks Formed by Associating Telechelic Chains. *Macromolecules* **2016**, *49*, 7510–7524.
- (20) Mordvinkin, A.; Döhler, D.; Binder, W. H.; Colby, R. H.; Saalwächter, K. Terminal Flow of Cluster-Forming Supramolecular Polymer Networks: Single-Chain Relaxation or Micelle Reorganization? *Phys. Rev. Lett.* **2020**, *125*, 127801.
- (21) Amin, D.; Wang, Z. Nonlinear rheology and dynamics of supramolecular polymer networks formed by associative telechelic chains under shear and extensional flows. *J. Rheol.* **2020**, *64*, 581–600.
- (22) Mohottalalage, S. S.; Senanayake, M.; Clemmer, J. T.; Perahia, D.; Grest, G. S.; O'Connor, T. Nonlinear Elongation Flows in Associating Polymer Melts: From Homogeneous to Heterogeneous Flow. *Phys. Rev. X* **2022**, *12*, 021024.
- (23) Senanayake, M.; Perahia, D.; Grest, G. S. Effects of interaction strength of associating groups on linear and star polymer dynamics. *J. Chem. Phys.* **2021**, *154*, 074903.

- (24) Ge, S.; Samanta, S.; Tress, M.; Li, B.; Xing, K.; Dieudonné-George, P.; Genix, A.-C.; Cao, P.-F.; Dadmun, M.; Sokolov, A. P. Critical Role of the Interfacial Layer in Associating Polymers with Microphase Separation. *Macromolecules* **2021**, *54*, 4246–4256.
- (25) Xing, K.; Tress, M.; Cao, P.; Cheng, S.; Saito, T.; Novikov, V. N.; Sokolov, A. P. Hydrogen-bond strength changes network dynamics in associating telechelic PDMS. *Soft Matter* **2018**, *14*, 1235–1246.
- (26) Ghosh, A.; Samanta, S.; Ge, S.; Sokolov, A. P.; Schweizer, K. S. Influence of Attractive Functional Groups on the Segmental Dynamics and Glass Transition in Associating Polymers. *Macromolecules* **2022**, *55*, 2345–2357.
- (27) Mitchell, G. R.; Odajima, A. The Local Conformation of Poly(dimethylsiloxane). *Polym. J.* **1984**, *16*, 351–357.
- (28) Wu, S. Phase structure and adhesion in polymer blends: A criterion for rubber toughening. *Polymer* **1985**, *26*, 1855–1863.
- (29) Kremer, F.; Schönhals, A. Broadband Dielectric Spectroscopy; Springer Science+Business Media, 2003.
- (30) Ferry, J. D. Viscoelastic Properties of Polymers; Wiley, 1980.
- (31) Tarnacka, M.; Jurkiewicz, K.; Hachuła, B.; Wojnarowska, Z.; Wrzalik, R.; Bielas, R.; Talik, A.; Maksym, P.; Kaminski, K.; Paluch, M. Correlation between Locally Ordered (Hydrogen-Bonded) Nanodomains and Puzzling Dynamics of Polymethysiloxane Derivative. *Macromolecules* **2020**, *53*, 10225–10233.
- (32) Ma, Y.; Lodge, T. P. Chain Exchange Kinetics in Diblock Copolymer Micelles in Ionic Liquids: The Role of χ . *Macromolecules* **2016**, 49, 9542–9552.
- (33) Wang, E.; Lu, J.; Bates, F. S.; Lodge, T. P. Effect of Corona Block Length on the Structure and Chain Exchange Kinetics of Block Copolymer Micelles. *Macromolecules* **2018**, *51*, 3563–3571.
- (34) Wang, E.; Zhu, J.; Zhao, D.; Xie, S.; Bates, F. S.; Lodge, T. P. Effect of Solvent Selectivity on Chain Exchange Kinetics in Block Copolymer Micelles. *Macromolecules* **2020**, *53*, 417–426.
- (35) Lu, J.; Bates, F. S.; Lodge, T. P. Chain Exchange in Binary Copolymer Micelles at Equilibrium: Confirmation of the Independent Chain Hypothesis. *ACS Macro Lett.* **2013**, *2*, 451–455.
- (36) Hansen, C. M. Hansen Solubility Parameters: A User's Handbook; CRC Press, 2007.
- (37) Stefanis, E.; Panayiotou, C. A new expanded solubility parameter approach. *Int. J. Pharm.* **2012**, 426, 29–43.
- (38) Tress, M.; Ge, S.; Xing, K.; Cao, P.-F.; Saito, T.; Genix, A.-C.; Sokolov, A. P. Turning Rubber into a Glass: Mechanical Reinforcement by Microphase Separation. *ACS Macro Lett.* **2021**, *10*, 197–202.